

# Theoretical Estimates of Mechanical Properties of the Endothelial Cell Cytoskeleton

Robert L. Satcher, Jr., and C. Forbes Dewey, Jr.

Fluid Mechanics Laboratory, Massachusetts Institute of Technology, Cambridge, Massachusetts 02139 USA

**ABSTRACT** Current modeling of endothelial cell mechanics does not account for the network of F-actin that permeates the cytoplasm. This network, the distributed cytoplasmic structural actin (DCSA), extends from apical to basal membranes, with frequent attachments. Stress fibers are intercalated within the network, with similar frequent attachments. The microscopic structure of the DCSA resembles a foam, so that the mechanical properties can be estimated with analogy to these well-studied systems. The moduli of shear and elastic deformations are estimated to be on the order of  $10^5$  dynes/cm<sup>2</sup>. This prediction agrees with experimental measurements of the properties of cytoplasm and endothelial cells reported elsewhere. Stress fibers can potentially increase the modulus by a factor of 2–10, depending on whether they act in series or parallel to the network in transmitting surface forces. The deformations produced by physiological flow fields are of insufficient magnitude to disrupt cell-to-cell or DCSA cross-linkages. The questions raised by this paradox, and the ramifications of implicating the previously unreported DCSA as the primary force transmission element are discussed.

## INTRODUCTION

Monolayers of endothelial cells change morphology when stimulated with laminar shear stress. After exposure, the individual cells are torpedo shaped, with the long axis aligned with the fluid flow vector (Dewey et al., 1981). Accompanying (and producing) this metamorphosis are changes in intracellular ionic flux (Shen et al., 1992; Sumpio et al., 1993); gene regulation, transcription, and translation (Resnick et al., 1993); and cytoskeletal structure (Davies, 1995; White et al., 1983; Levesque et al., 1986). The mechanism by which cells detect shear stress is undefined. The cells must be deformed; however, mechanical properties are poorly understood. The difficulty with determining how endothelial cells respond to force has been due in large part to lack of a description of the precise architecture of the cell cytoskeleton and its enclosing membrane.

The endothelial cell has a cytoskeleton composed of three polymers: F-actin, intermediate filaments, and microtubules. As the structural backbone, it perhaps allows the cell to detect forces by deformations and/or distortions at the membrane interface. Each component of the cytoskeleton has been studied by immunofluorescence, confirming that structure is altered when endothelial cells respond to shear stress (Gotlieb et al., 1991; Satcher et al., 1992). The most prominent documented changes occur with microfilaments (Lewis and Lewis, 1924; White et al., 1983). F-actin comprises a large percentage of the total protein in endothelial cells (Satcher, 1993) and is organized and used in various ways.

Actin is utilized by cells for stability, mobility, and force generation (Ettenson and Gotlieb, 1992; Kreis and Birnmeier, 1980). Cross-linked F-actin microfilaments form the distributed cytoplasmic structural network (DCS network) that fills the cytoplasm (Satcher, 1993). Microfilaments are also grouped together with myosin and other actin-binding proteins to form 200–500-nm-diameter bundles called “stress fibers.” The cell controls actin via a large armament of regulatory proteins, which shift actin between the polymeric and monomeric (G-actin) pools as required. The assumed function of stress fibers is to reinforce the cell against surface shearing forces applied by blood flow (White et al., 1983; Wang et al., 1994a; Satcher et al., 1992). However, it is difficult to prove this while lacking knowledge of force transmission through endothelial cells. In previous work, we observed that the F-actin cytoskeleton and stress fibers are arranged in a configuration consistent with a force-bearing role (Satcher, 1993). In this paper we explore the possibility that forces distort the microfilament network, and the related question of whether stress fibers afford any mechanical advantage.

There are earlier models of the mechanical properties of the cytoskeleton. Measurements have been made using techniques such as micropipette aspiration (Sato et al., 1987) and magnetometry (Wang et al., 1994a) to deform cells and infer mechanical properties. Theoretical treatments were offered by Fung and Liu (1993), Wang et al. (1994b), and Theret et al. (1988). However, these estimates were hindered by experimental limitations and lack of detailed information about cytoskeletal ultrastructure. For example, Sato et al. (1987) made measurements of mechanical properties using micropipette aspiration. Theret et al. (1988) constructed a model from these measurements to estimate the elastic modulus of the cortical cytoplasm based on the observed length of cell sucked into the micropipette by a specified pressure differential. To manipulate the cells, it was necessary to detach cells from monolayers using chem-

*Received for publication 4 October 1995 and in final form 18 March 1996.*

Address reprint requests to Dr. Robert L. Satcher, Jr., Fluid Mechanics Laboratory, 3–250, Massachusetts Institute of Technology, Cambridge, MA 02139. Tel.: 617-253-2235; Fax: 617-258-8559; E-mail: basacher@itsa.ucsf.edu.

© 1996 by the Biophysical Society

0006-3495/96/07/109/10 \$2.00

icals that are known to disrupt F-actin. Moreover, the model proposed by Theret was not based on detailed ultrastructural information. Wang et al. (1994a) proposed that the endothelial cell cytoskeleton can be characterized as a tensigrity structure. By deforming the cell surface with magnetic beads bound to the extracellular matrix receptor integrin  $\beta_1$ , they showed that the measured stiffness increased with applied stress. If stresses are transmitted directly to the cytoskeleton by receptors, this is a good measure of mechanical properties. According to the tensigrity model, F-actin filaments produce tension, which is partially supported by microtubules in compression. The model is primarily based on the observation that endothelial cells exert tension on the underlying substrate (Wang et al., 1994b). There is indirect evidence with fibroblasts to support this hypothesis: disruption of microtubules causes an increase in tension exerted on the substrate (Kolodney and Wysolmerski, 1992). However, there is no corroborating evidence for endothelial cells; and the intracellular architecture predicted by this model has not been demonstrated experimentally. Fung and Liu (1993) consider shear stress in their model. A framework is established for analyzing the intracellular stress distribution, and a detailed calculation is performed for the limiting case of the cell membrane acting as the exclusive force-bearing structure in the cell. The opposing case of load bearing by the cytoplasm structure is not analyzed, because of a lack of detailed information about the mechanical properties of cytoplasm in endothelial cells.

In the present study, we use prior observations (Satcher, 1993) of the endothelial cytoskeleton with high-resolution three-dimensional electron microscopy to estimate mechanical properties. Elastic moduli for shear and tension/compression are computed and compare favorably with experimental data. F-actin bundles constructed in response to shear stress would be expected to reinforce the cortical network in the presence of laminar shear stress, reducing deformability and stabilizing the cell-cell attachment configuration.

## MATHEMATICAL MODEL AND METHODS

### Cell environment

Endothelial cells form a monolayer that covers the innermost aspect of arteries, serving as a barrier between flowing blood and artery wall. Individual cells have a profile similar to that of an egg that is sunny side up. They are flat except for a slight bulge caused by the nucleus. As illustrated in Fig. 1, flowing blood contacts the luminal surface of the monolayer. The artery wall beneath the monolayer is deformed by fluid stress directed normal to the surface. However, it is reasonable to assume that the shear modulus of the artery wall is much larger than the monolayer (Dewey, 1979). Thus, the endothelial monolayer is deformed more than the artery wall by shear stress. Cells grown for *in vitro* studies are affixed to a rigid glass coverslip on which

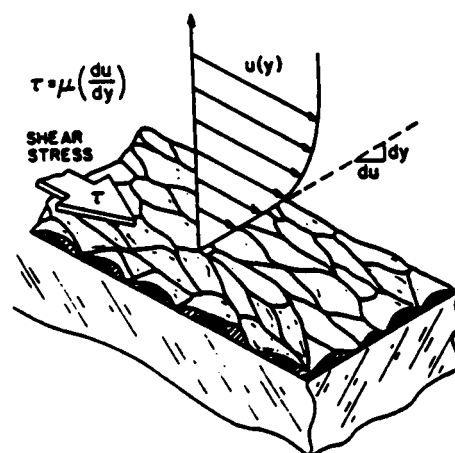


FIGURE 1 Schematic diagram of endothelial monolayer (adapted from Dewey et al., 1981). Direction of fluid flow is indicated by arrow. The cells are adherent to substrate below, so that shear stress imparted by the flow field is transmitted to basal membrane attachment points.  $\mu$  = fluid viscosity.

glycoproteins (such as vitronectin, fibronectin, and laminin) are layered by the cells themselves.

Shear stress is transmitted through cells from the apical membrane to substrate by intervening structures (the cytoskeleton, cytoplasm, nucleus, etc.). Intracellular mechanical properties are therefore a composite of the characteristics of constituent filaments, cytoplasm, membrane, and organelles. But F-actin is the most likely load-bearing structure for surface forces. The cortical cytoskeleton is predominantly constructed from F-actin. It attaches to the apical and basal cell membranes. There are specific differences in F-actin configuration between aligned and nonaligned cells, including a reorganized distributed cytoplasmic structural actin (DCSA) network and the presence of stress fibers with apical attachments in aligned cell (Gotlieb et al., 1991; Satcher, 1993). In sheared cells intermediate filaments and microtubules are found in increased densities near the nucleus, but they appear at lower frequency than F-actin in most regions (Satcher, 1993). Moreover, solutions of intermediate filaments and microtubules have a lower mechanical modulus than solutions of F-actin, fluidizing at lower strains (Janmey et al., 1991). We will determine the mechanical properties of the F-actin cytoskeleton by creating a model based on ultrastructural detail. The results are compared with experimental measurements of endothelial cell mechanical properties.

### F-ACTIN MODEL

The endothelial cytoskeletal network resembles the microscopic structure of various natural and synthetic materials, including wood, cancellous bone, coral, glass foams, bread, cornflakes, and paper, to name a few (Fig. 2). The F-actin cytoskeleton is an open lattice, formed from interconnected solid struts or fibers. Small deformations of this lattice occur

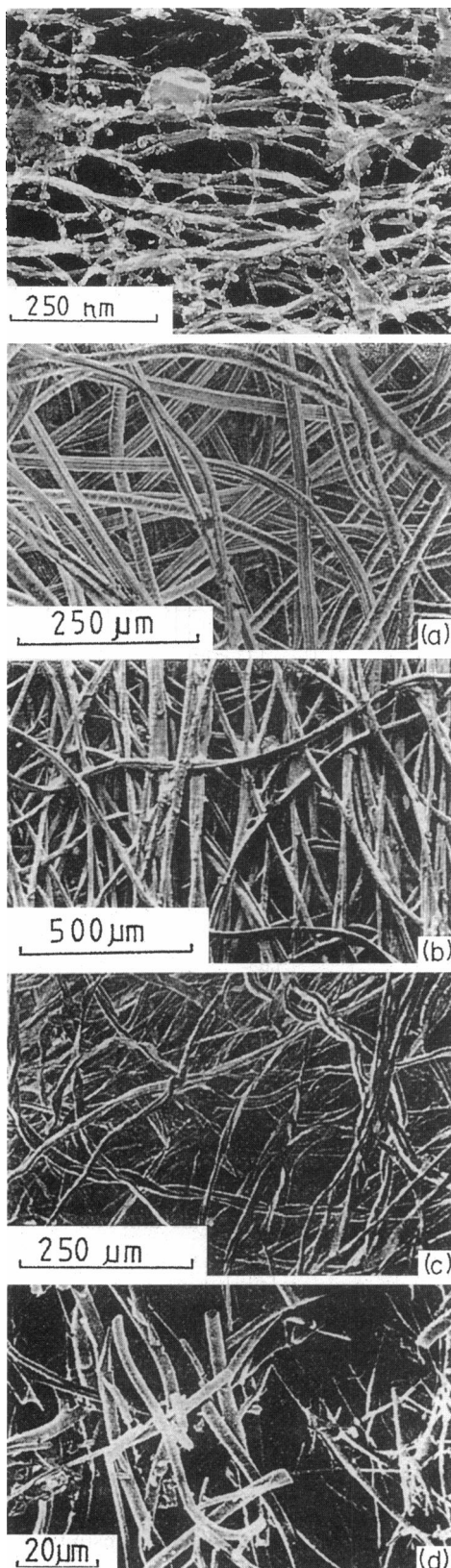


FIGURE 2 Comparison of endothelial cytoskeleton (top picture) with various "cellular solids": (a) Felt, (b) paper, (c) cotton wool, (d) space shuttle tile. The microscopic structure is similar, because the distributed cytoplasmic structural actin network is formed by cross-linked actin fibers (adapted from Gibson and Ashby, 1988).

by bending, stretching, and twisting of constituent fibers. Thus, mechanical properties should be derivable from constituent material mechanical properties and lattice geometry. There are errors immediately apparent from this approach, because the F-actin cytoskeleton is a dynamic system and is interconnected to microtubules and intermediate filaments (Runge et al., 1981). Moreover, the cross-links between F-actin fibers themselves are heterogeneous and would be expected to vary in binding strength. But we will postpone consideration of these factors until the end of our analysis, as it does not alter the fundamental premise of the model.

The geometry of the network has primary, secondary, and tertiary levels of organization. At the lowest level, fibers are constructed from F-actin monomers. At the secondary level, fibers are cross-linked to form a porous network and to form bundles. At the highest level, the network of fibers and bundles surrounds organelles, fills the space between luminal and basal cell membranes, and forms complex interactions with the nucleus and membrane proteins. Forces transmitted from the cell surface would affect the lattice geometry at all levels. The F-actin network would be deformed by various mechanisms, including linear elastic and/or plastic processes.

We borrow from the analysis of "cellular solids" (Gibson and Ashby, 1988) to proceed. Most lattice-like materials in tension and compression exhibit stress-strain relationships with two discernible regions: 1) linear elasticity at low stress, where deformation occurs by filament bending, stretching, or twisting. Elastic deformations are reversible—energy imparted to the material is stored and recovered when the material returns to its original shape. The Young's and shear moduli of the constitutive material determine the slope of the stress-strain curve for the lattice; and 2) plasticity at higher stress, where deformation is by elastic buckling, plastic hinging, and brittle crush and fracture of filaments. Plastic deformations are dissipative—energy causes irreversible deformations of the material. If the network is fluid filled (as in cells with cytoplasm), viscous work must be performed to move fluid in addition to deforming the lattice. This tends to increase the dynamic stiffness. Modeling based on this approach has yielded accurate scaling laws for a wide variety of materials (Fig. 3), because for small lattice deformations, the precise arrangement of filaments is not critical (Gibson and Ashby, 1988). The integrated response of the network is primarily a function of the amount of material per unit volume and (of course) the type of material. Consequently, analysis of a complicated open lattice such as the endothelial cytoskeleton can be approached by choosing an array that has similar spatial density and arrangement of filaments, and in which network deformations are produced by the same microscopic processes of filament bending, stretching, twisting, and so forth. Such a network should exhibit the same or similar macroscopic behavior within a range of small deformations.

We choose the configuration illustrated in Fig. 4, an array of filaments of length 1 and square cross section of side  $t$ .

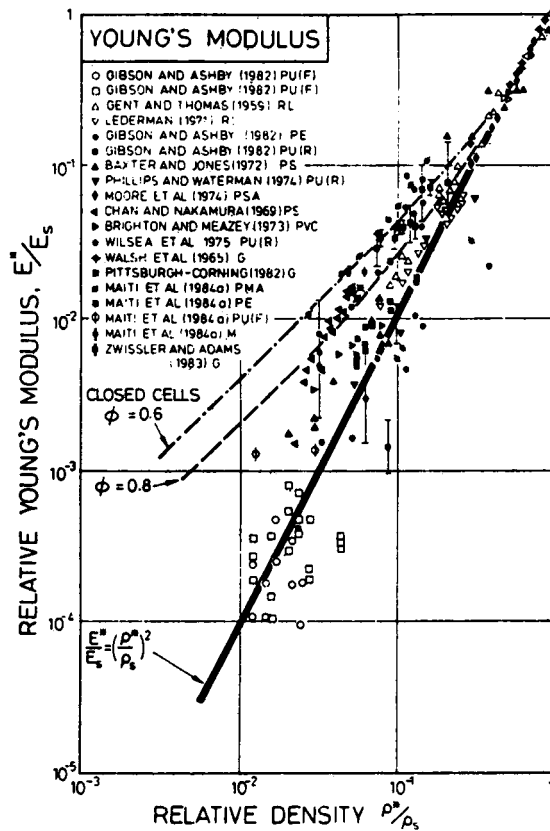


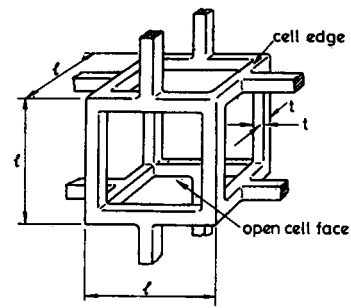
FIGURE 3 Moduli versus relative density. Data for the relative Young's modulus of foams are plotted against relative density. The solid line represents the theory for open cell foams (adapted from Gibson and Ashby, 1988).

This configuration has been used with success in previous problems (Gibson and Ashby, 1988) of elastic and plastic deformation of forms. Adjoining network "cells" are staggered, so that members meet at their midpoints. Note that the endothelial cytoskeleton connectivity and geometry are much more complex. But the model geometry captures the assumed response of the real network: deformations are produced by bending or stretching of constituent filaments. Analysis is facilitated by the simple arrangement of the elements. Future work can adopt more complicated junction geometries.

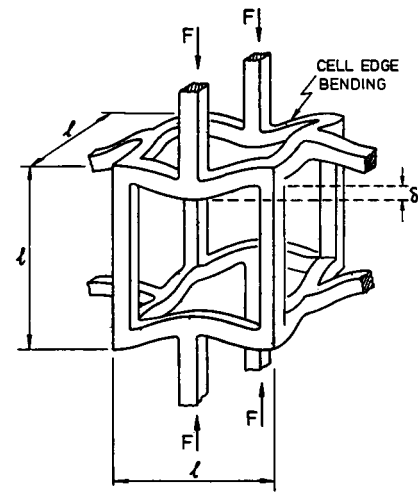
### Characterization of mechanical properties

Mechanical properties can be expressed in terms of quantities such as density and moment of inertia, which can be difficult to determine for complex materials such as the F-actin cytoskeleton. However, by using a nondimensional form, we are able to express network parameters in terms of constituent filament properties and empirical constants. We define the relative density:

$$\frac{\rho^*}{\rho_s} \equiv \text{relative density,}$$



(a)



(b)

FIGURE 4 (a) Unit cell of open-lattice model for cytoskeleton. (b) Loading of unit cell due to shear stress, indicating mechanism of deformation due to transmitted force,  $F$  (Gibson and Ashby, 1988).

where  $\rho^*$  is the average density of the network, and  $\rho_s$  is the density of the constituent filaments (in our case F-actin). The relative density is related to the unit cell dimensions by

$$\frac{\rho^*}{\rho_s} \propto \left\{ \frac{l}{l} \right\}^2. \quad (1)$$

If we consider the filaments to be beams, the moment of inertia is related according to

$$I \propto l^4. \quad (2)$$

Young's modulus is calculated by considering a mechanical deformation of the network. A uniaxial loading on the network causes each unit cell edge to transmit a force  $F$ , as illustrated in Fig. 4 b. The beams of length  $l$  are loaded at their midpoints with force  $F$ . The consequent linear-elastic deflection of the unit cell structure is estimated as

$$\delta \propto \frac{F l^3}{E_s I}, \quad (3)$$

where  $E_s$  is Young's modulus of the beams (filaments), and  $\delta$  is the linear-elastic deflection.  $F$  is related to the remote compressive stress on the network,  $\sigma$ , by

$$F\alpha\sigma l^2, \quad (4)$$

and the strain  $\varepsilon$  is related to unit cell displacement  $\delta$  by

$$\varepsilon\alpha\frac{\delta}{l}. \quad (5)$$

For the network, Young's modulus is defined as

$$E^* \equiv \frac{\sigma}{\varepsilon} = \frac{C_1 E_s I}{l^4}, \quad (6)$$

where  $C_1$  is a constant. Substituting Eqs. 1 and 2 in 6, we get

$$\frac{E^*}{E_s} = C_1 \left\{ \frac{\rho^*}{\rho_s} \right\}^2 \quad (7)$$

For the shear modulus,  $G^*$ , we consider a shear stress  $\tau$  applied to the network, causing strain  $\gamma$ . Unit cell members respond as before by bending, so that

$$\tau\alpha\frac{F}{l^2}; \quad \gamma\alpha\frac{\delta}{l}, \quad (8)$$

and  $\delta$  is given by Eq. 3. Now,

$$G^* = \frac{\tau}{\gamma} = \frac{C_2 E_s I}{l^4}. \quad (9)$$

Substituting Eqs. 1 and 2 in 9, we get

$$\frac{G^*}{E_s} = C_2 \left\{ \frac{\rho^*}{\rho_s} \right\}^2. \quad (10)$$

Data are available for Young's and shear moduli for materials with a wide range of relative densities (Fig. 3). The best fit is for  $C_1 \approx 1$ ;  $C_2 \approx 3/8$  (Gibson and Ashby, 1988). Therefore,

$$\frac{G^*}{E_s} \approx \frac{3}{8} \left\{ \frac{\rho^*}{\rho_s} \right\}^2; \quad \frac{E^*}{E_s} \approx \left\{ \frac{\rho^*}{\rho_s} \right\}^2. \quad (11)$$

## RESULTS

### F-actin network properties

To estimate  $G^*$  and  $E^*$  for a network of F-actin, we must first know  $\rho^*$ ,  $\rho_s$ , and  $E_s$ . Density data for F-actin indicate (CRC Handbook of Biochemistry)

$$\rho_s = 732 \text{ mg/ml}$$

For a second estimate, x-ray crystallography studies show (Taniguchi et al., 1983) that the unit cell of crystalline G-actin contains one molecule (MW 42,500) and has dimensions  $a = 61 \text{ \AA}$ ;  $b = 41 \text{ \AA}$ ;  $c = 33 \text{ \AA}$ ; and  $\alpha = \beta = \gamma = 90^\circ$ . The computed density is  $\rho_s = 845 \text{ mg/ml}$ . For the average network density, various investigators estimate that the concentration of F-actin in the cyto-

plasm of eukaryotic cells is  $\rho^* = 10\text{--}20 \text{ mg/ml}$  (Hartwig et al., 1989; Stossel et al., 1988). We measure the F-actin content of nonoriented bovine aortic endothelial cells at  $\sim 10 \text{ mg/ml}$ . The relative density is therefore approximately 1%.

Young's modulus of F-actin is estimated from the bending modulus,  $\Gamma$  (Osawa, 1977; Kishino and Yanagida, 1988), using the relation  $E_s = \Gamma/l$ . For F-actin,  $\Gamma = 1.7 \times 10^{-17} \text{ dyne-cm}^2$ ; and  $I = \pi a^4/4$  for a cylinder of radius  $a$ . Using  $a = 3.5 \text{ nm}$ , we get  $E_s = 1.442 \times 10^9 \text{ dyne/cm}^2$ . Substituting these values in Eq. 11, we get

$$E^* \approx O(10^5 \text{ dyne/cm}^2) = O(10^4 \text{ N/m}^2)$$

and

$$G^* \approx O(10^5 \text{ dyne/cm}^2) = O(10^4 \text{ N/m}^2) \quad (12)$$

In Table 1, we compare computed values with experimental measurements of the elastic shear modulus. Various experimental schemes were used on solutions of pure F-actin, whole cells, and cytoplasm by different investigators. Our estimates compare favorably with F-actin solutions of concentration approaching  $10 \text{ mg/ml}$  and with cytoplasm, in both cases giving the same order of magnitude for the modulus of elasticity. It should be noted that the experiments were performed for small deformations of the material of interest.

### Network properties with stress fibers

Stress fibers could conceivably act in parallel or in series to the cortical cytoskeleton, transmitting luminal surface loads to substrate and intercellular attachments. Both cases are considered, because the connectivity is uncertain, and to illustrate that the result is essentially independent of this choice. We can estimate the effects of stress fibers via a simple model (Fig. 5). In Fig. 5 A, the stress fiber (element 2) is in parallel with the actin network (element 1). In Fig. 5 B, they are arranged in series.

#### Parallel elements in tension

Consider element 1 in parallel with element 2, with tensile force  $T$  applied to the composite structure (Fig. 6). System constraints are expressed as

**TABLE 1** Computed and experimental estimates of elastic shear modulus

Reference	Material	Concentration (mg/ml)	Elastic modulus (dynes/cm <sup>2</sup> )
Janmey et al., 1991	F-actin	10	$10^4\text{--}10^5$ (shearing)
Adams, 1992	Cytoplasm	—	$\sim 10^5$ (stretching)
Theret et al., 1988	Nonoriented BAEC	—	$\sim 10^3$
	Oriented BAEC	—	$\sim 10^4$

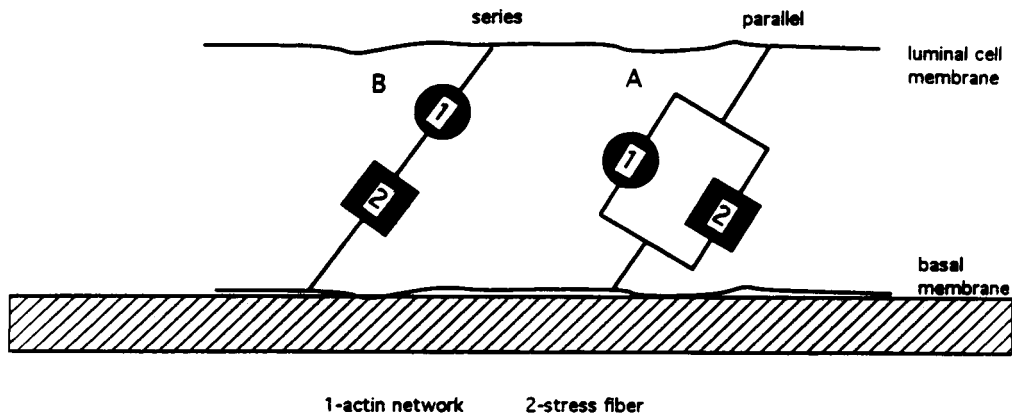


FIGURE 5 Schematic of stress fibers as (A) parallel and (B) series elements with cortical actin network for the case of tensile loading.

$$T_1 + T_2 = T \text{ and } \varepsilon_1 = \varepsilon_2 = \varepsilon, \quad (13)$$

where  $T_n$  is the tension in element  $n$ ; and  $\varepsilon_n$  is the strain in element  $n$ . For the composite structure,

$$\sigma = \frac{T}{A} = \frac{T_1 + T_2}{A}, \quad (14)$$

where  $A$  is the relevant membrane area;  $\sigma$  is the stress on the membrane. Thus, the effective parallel modulus,  $E_p$ , is

$$E_p = \frac{\sigma}{\varepsilon} = \frac{T_1 + T_2}{\varepsilon A} = \frac{A_1 \sigma_1 + A_2 \sigma_2}{\varepsilon A} = \frac{A_1 E_1 + A_2 E_2}{A}, \quad (15a)$$

where  $\sigma_n$  is the stress in element  $n$ . In condensed notation,

$$E = \sum_{n=0}^m \frac{A_n E_n}{A}. \quad (15b)$$

The contributions of constituent moduli to the composite modulus are additive for parallel elements.

#### Series elements in tension

Now consider element 1 in series with element 2, with tensile force  $T$  applied (Fig. 7). The constraining equations are now

$$T = T_1 = T_2 \text{ and } \Delta l = \Delta l_1 + \Delta l_2. \quad (16)$$

Thus,

$$\varepsilon = \frac{\Delta l}{l} = \frac{\Delta l_1 + \Delta l_2}{l} = \varepsilon_1 \frac{l_1}{l} + \varepsilon_2 \frac{l_2}{l}, \quad (17)$$

substituting for  $\varepsilon_n$ ,

$$\varepsilon = \frac{\sigma_1 l_1}{E_1 l} + \frac{\sigma_2 l_2}{E_2 l} = \frac{T l_1}{A_1 E_1 l} + \frac{T l_2}{A_2 E_2 l}, \quad (18)$$

and substituting  $T = A\sigma$ , we obtain

$$\varepsilon = \left\{ \frac{A l_1}{A_1 l E_1} + \frac{A l_2}{A_2 l E_2} \right\} \sigma. \quad (19)$$

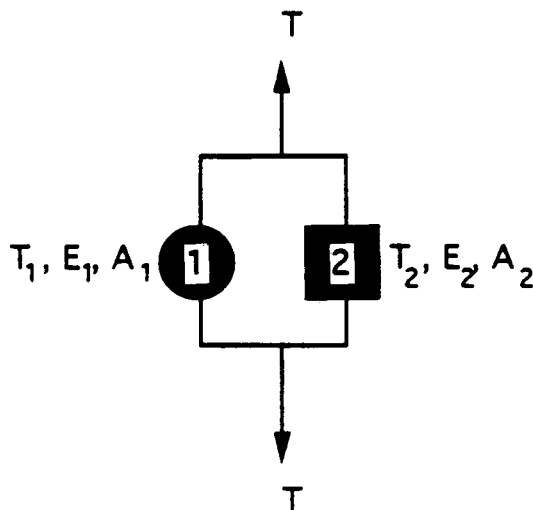


FIGURE 6 Parallel elements loaded with tensile force,  $T$ .

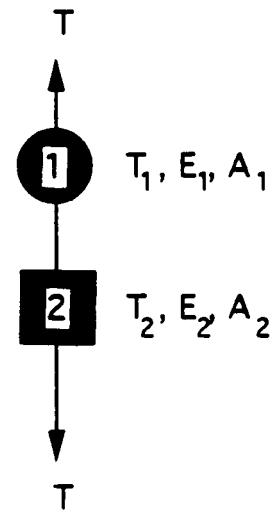


FIGURE 7 Series elements loaded with tensile force,  $T$ .

For the composite structure with series elements, the equivalent elastic modulus is

$$E_s = \frac{\sigma}{\varepsilon}, \quad (20)$$

and substituting Eq. 19 in Eq. 20, we get

$$\frac{1}{E_s} = \frac{Al_1}{A_1lE_1} + \frac{Al_2}{A_2lE_2}, \quad (21)$$

or in condensed notation,

$$\frac{1}{E_s} = \frac{A}{l} \sum_{n=1}^m \frac{l_n}{A_n E_n}. \quad (22)$$

Thus, to obtain the composite modulus for series elements we add the inverse of constituent moduli.

In the case of series elements (Eq. 22), and with parallel elements (Eq. 15), the respective constituent moduli  $E_p$  and  $E_s$  are scaled by the area ratio  $A_n/A$ . These ratios can be estimated either directly, or by using a scaling argument. Endothelial cells typically have  $\sim 10$  stress fibers per cell (Gotlieb et al., 1991), comprising less than 1% of the total F-actin mass (Satcher, 1993). If we assume that each connects to the luminal membrane, the force on 1/10 of the luminal membrane (on average) is the relevant tension for the series and parallel elements of Figs. 6 and 7. Thus, the area of the membrane,  $A$ , is 1/10 the total luminal membrane area. Next, we equate the network area ( $A_1$ ) to  $A$ , because the tensile force will be resisted by network beneath the membrane with equivalent cross-sectional area. Finally, we estimate the cross-sectional area of a stress fiber from morphological data. A typical stress fiber is 0.2–0.4  $\mu\text{m}$  in diameter. The cross section is idealized as a circle. The elastic modulus of the network is known (Table 1); and the modulus of stress fibers is assumed to be the same as that of F-actin. These values are substituted in Eqs. 15a and 21 to obtain the effective moduli  $E_p$  and  $E_s$  (Table 2).

We can alternatively estimate the area ratio based on the numbers of F-actin filaments and stress fibers. It can be argued that the area ratio  $A_2/A_1$  scales as the ratio of filament numbers (because network properties are determined by the density of filaments). Thus,  $A_2/A_1 = N(\text{stress fibers})/N(\text{F-actin filaments}) = 10/10^5 = 10^{-4}$ . The predicted Young's modulus is included in Table 2.

$$\frac{E_s}{E_n} \approx \frac{10^9}{10^5} = 10^4,$$

where the subscript designations are n, network; s, stress fibers; c, composite element. From direct area estimate:

$$\frac{A_s}{A_c} = \frac{A_s}{A_n} \approx 10^{-3}.$$

**TABLE 2 Stress fiber enhancement of network strength**

Type	Area ratio estimate	Computed modulus ratio ( $E_c/E_n$ )
Parallel	Direct	11
	Number density	2
Series	Direct	1.8
	Number density	1

From number density:

$$\frac{A_s}{A_n} \approx 10^{-4}.$$

In all cases except for the last, stress fibers significantly enhance the Young's modulus. There is more augmentation with the parallel arrangement than with the series arrangement.

Finally, if we estimate the network strain (without stress fibers) using physiological levels of shear stress (20 dynes/cm<sup>2</sup>) (Dewey, 1979),

$$\varepsilon = \frac{\tau}{E^*} = 10^{-4} \text{ (0.01\%)}. \quad (23)$$

This is a surprising result—a deformation of 0.01% is probably too small to affect network cross-links and therefore would not be expected to directly disrupt filament-filament interactions. In addition, a cell would not be displaced significantly for this degree of deformation, so that it is highly unlikely that cell-cell contacts are directly affected.

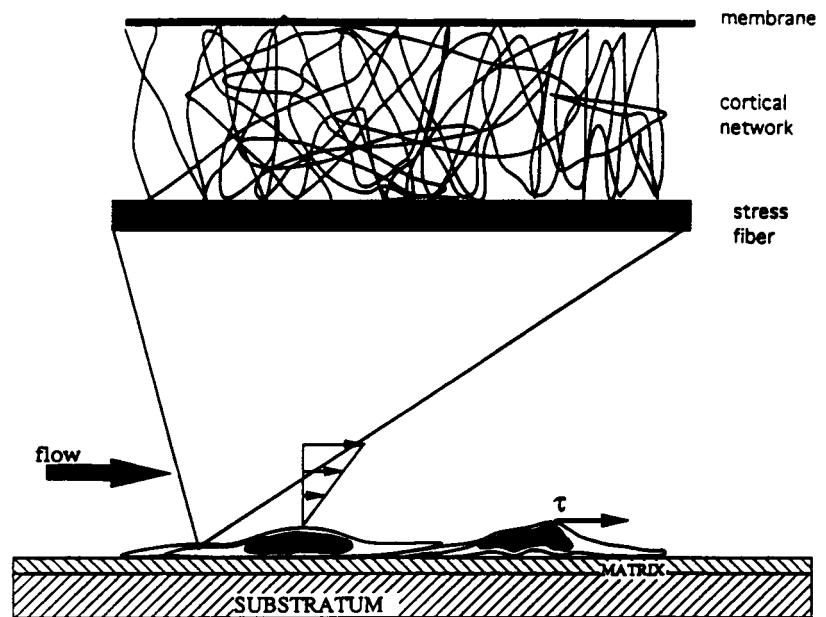
#### Elements in shear

Stress fibers in apical regions might reduce the deformation caused by shear stress. To evaluate this effect, we consider series and parallel elements with shear loading. Analysis yields the same equations as for tensile loading (see Eqs. 15 and 21). Stress fibers in aligned cells are located just below the top membrane (Satcher, 1993), where they appear to attach. The length of aligned BAEC (typical length  $\sim 40 \mu\text{m}$ ) is much more than the apical/basal thickness ( $< 1.0 \mu\text{m}$ ). Stress fibers can extend for the length of a cell (Satcher, 1993); thus, they are essentially parallel to the top membrane. Actin filaments branch from stress fibers and attach to the surrounding cortical network along the entire length of the fiber (Satcher, 1993). This is represented schematically in Fig. 8. The shear modulus of stress fibers is assumed to be identical to F-actin ( $\sim 10^9$  dynes/cm<sup>2</sup>), which is much more than the shear modulus of the network ( $0.9 \times 10^5$  dynes/cm<sup>2</sup>). Without stress fibers the deformation angle,  $\gamma$ , is (see Fig. 9)

$$\gamma = \frac{\tau}{G} = 2 \times 10^{-4} \text{ radians (0.01\%)}$$

A for  $\tau = 20$  dynes/cm<sup>2</sup>. This is a physiologically insignificant deformation. Thus stress fibers acting in parallel,

FIGURE 8 Schematic of stress fiber beneath top membrane, with many attachments to intervening distributed cytoplasmic structural actin network.



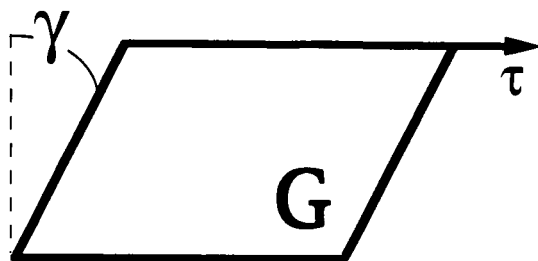
series, or any conceivable arrangement would have a vanishing and probably irrelevant effect on reducing network deformation with comparable levels of shear stress.

## DISCUSSION AND CONCLUSIONS

Vascular endothelium grows as a monolayer of cells on the innermost aspect of the artery wall. As the interface between flowing blood and artery, the endothelial cells are able to withstand shear stress without mechanical damage. Cells are attached to the substrate below and neighboring cells on the sides. Forces on the luminal cell membrane are transmitted to basal attachment sites. It had been postulated that

this occurs via tension in the cell membrane (Fung and Liu, 1993). However, from three-dimensional ultrastructural studies, the cytoskeleton was identified as the probable load-bearing element in endothelium (Satcher, 1993). In endothelial cells, F-actin is organized as the distributed cytoplasmic network and as stress fibers. Other cells such as erythrocytes and platelets utilize an additional distinct sub-membranous network composed of F-actin to support the membrane and interface with the cytoskeleton. As with macrophages (Hartwig et al., 1988), this network does not exist in endothelial cells. Rather, the distributed cytoskeleton of endothelial cells appears to directly attach to the luminal and basal membranes (Satcher, 1993). Stress fibers attach to focal adhesions, and probably with the luminal membrane in aligned cells. And there are many connections between the DCSA and stress fibers. Thus force transmission proceeds from surface to F-actin cytoskeleton to substrate.

Our findings and observations of others are consistent with the cytoskeleton serving as the stress-bearing element (Dewey et al., 1981; Hartwig et al., 1991; Wong et al., 1983; White et al., 1983). Shear stresses are transmitted via the cytoskeleton-to-substrate attachments (Davies et al., 1994). Fung proposed that shear stress is transmitted via the cell membrane itself to substrate attachments (Fung and Liu, 1993). However, there are many attachment points between the F-actin cytoskeleton and the cell membrane (Satcher, 1993). Because the membrane only carries stress built up between attachments, the membrane levels would be low and perhaps insignificant. The bulk elastic shear and compressive/tension moduli were estimated by using the theory of foams (Gibson and Ashby, 1988). This approach uses simplifying assumptions concerning the cross-linking (Nossal, 1988) and the geometry of the F-actin network. However, calculated values are in good agreement with experi-



$\tau$  - shear stress

$G$  - shear modulus

$\gamma$  - deformation angle

FIGURE 9 Schematic of deformation angle caused by uniaxial shear stress  $\tau$ , on element of shear modulus  $G$ .



mental measurements on cytoplasm and F-actin gels (Table 1) (Janmey et al., 1994). Physiological forces do not significantly deform the DCSA. Stress fibers would help to reinforce this network, effectively increasing the modulus in the vicinity of their attachments to the luminal membrane. However, predicted deformations are so small that cell-to-cell contact regions and DCSA cross-linkages are unaffected. Therefore, the role of stress fibers for mechanotransduction is unclear. As discussed below, the alignment of stress fibers with the flow axis may be an intermediate stage that facilitates the metamorphosis to the flow-induced state.

The transduction mechanism for shear stress is unknown. Others have postulated the existence of stretch receptors and stretch sensitive channels in the luminal cell membrane (Harrigan, 1990; Sachs, 1988). Our findings are consistent with the existence of signaling proteins that are sensitive to deformation. A protein that links the cytoskeleton to the luminal membrane could serve this function. There are discrete areas where the cytoskeleton is attached to the overlying membrane. In other cell types (platelets and erythrocytes) these linkages have been identified and studied extensively (Hartwig et al., 1989; Fox, 1985; Lux, 1979; Branton et al., 1981). Constituent proteins that compose these complexes include actin-binding protein (ABP), spectrin, and integral membrane proteins such as GP IX-1b. Endothelial cells may use these and other molecules for the linkage (Gorlin et al., 1990). Shearing forces would displace the luminal membrane relative to the cytoskeleton, so that the linkage molecules would be deformed, perhaps causing  $\text{Ca}^{2+}$  or  $\text{K}^{+}$  currents in response (Shen et al., 1992).

In the case of laminar flow, transcellular stress fibers are constructed as cells orient in the direction of flow. Buxbaum et al. (1987) have performed experiments showing that cytoplasm of some cells behaves as a thixotropic viscoelastic material in vitro—it deforms elastically until a critical yield stress is reached, then flows as an indeterminate fluid. The shear stress in flowing cytoplasm is independent of shear rate, because there is an inverse proportionality between viscosity and shear rate (Buxbaum et al., 1987). The yield stress of F-actin solutions in shear (of  $\sim 10$  mg/ml, the concentration of cytoplasm) is on the order of dynes/cm<sup>2</sup> (Kerst et al., 1990). The threshold shear stress for endothelial cell alignment is  $\sim 8$  dynes/cm<sup>2</sup> (Dewey et al., 1981). From our previous calculations, we know that gradients of  $\sim 40\%$  of average shear stress occur across the monolayer due to the protrusion of the nuclear bulge into the fluid stream (Satcher et al., 1992). The cytoplasm may begin to flow at the points of highest shear stress, causing the alignment of F-actin network fibers and subsequent construction of stress fibers. Because stress fibers increase the modulus of the network locally, the cytoplasmic streaming would be self-limited, stopping soon after stress fibers achieve their final length. When purified actin gels are subjected to shear stress, regions of aligned fibers aggregate to form a crystalline phase that is very similar in morphology to stress fibers (Cortese et al., 1988; Suzuki et al., 1989; Buxbaum et al., 1987; Ito et al., 1987). Moreover, ultrastructural studies

show that many stress fibers in oriented cells tend to have one attachment at or around the nucleus, where stresses would be at a maximum (Satcher, 1993).

Further studies are needed to assess the structural model proposed here. The distribution and length of stress fibers in three dimensions should be quantified. In addition, F-actin filaments probably interact with microtubules and intermediate filaments. These proteins may bond F-actin filaments to each other at points of close proximity, decreasing the effective actin filament lengths. Our model does not account for such bridging, in part because the precise nature of interfilament interactions is unknown. The role of F-actin in alignment has been studied, but little is known about the role of intermediate filaments or microtubules for normal adjustments. The tensigrity model proposes that the F-actin cytoskeleton is maintained in a constant state of tension, using microtubules to support the compressive load (Wang et al., 1994). Our model does not invalidate this hypothesis, but in contrast to tensigrity structures, interfilament tension is not required to explain observed adjustments in response to shear stress. Moreover, ultrastructural observations show that the density of microtubules in cytoplasm is much less than that of F-actin. The role of intermediate filaments and microtubules could be tested by observing alignment in the presence of agents that disrupt these filament systems.

Our model also does not explain endothelial response to turbulent flow (Davies et al., 1986). In this case, cells respond by dividing at average shear stresses below those needed to align cells ( $\sim 2\text{--}3$  dynes/cm<sup>2</sup>). An unknown system detects the inherent and intermittent chaotic variations in shear stress with turbulent flow. Further studies of cells in these conditions are needed to identify the mechanism involved.

In conclusion, the theory of foams offers a means of modeling the mechanical properties of the distributed cytoplasmic structural actin network (DCSA). The predicted modulus of elasticity agrees with experimental measurements of cytoplasm and endothelial cells reported elsewhere. Stress fibers enhance the rigidity of the DCSA; however, deformations produced by physiological flow fields are too small to affect cell attachments or DCSA cross-linkages. More studies are needed to investigate the role of stress fibers in cells.

## REFERENCES

- Adams, D. S. 1992. Mechanisms of cell shape change: the cytomechanics of cellular response to chemical environment and mechanical loading. *J. Cell Biol.* 112:83–93.
- Branton, D. C., C. M. Cohen, and J. Tyler. 1981. Interaction of cytoskeletal proteins on the human erythrocyte membrane. *Cell.* 24:24–32.
- Buxbaum, R. E., T. Dennerll, S. Weiss, and S. R. Heidemann. 1987. F-actin and microtubule suspensions as indeterminate fluids. *Science.* 235:1511–1514.
- Cortese, J. D., and C. Frieden. 1988. Microheterogeneity of actin gels formed under controlled linear shear. *J. Cell Biol.* 107:1477–1487.
- Davies, P. F. 1995. Flow-mediated endothelial mechanotransduction. *Physiol. Rev.* 75:519–560.

- Davies, P. F., A. Remuzzi, E. J. Gordon, C. F. Dewey, and M. A. Gimbrone. 1986. Turbulent fluid shear stress induces vascular endothelial cell turnover in vitro. *Proc. Natl. Acad. Sci. USA*. 83:2114-2117.
- Davies, P. F., A. Robotenskyj, and M. C. Griem. 1994. Endothelial cell adhesion in real time measurements in vitro by tandem scanning confocal image analysis. *J. Clin. Invest.* 93:2031-2038.
- Dewey, C. F., Jr. 1979. Fluid mechanics of arterial flow. *Adv. Exp. Med. Biol.* 115:55-103.
- Dewey, C. F., S. Bussolari, M. Gimbrone, and P. F. Davies. 1981. The dynamic response of vascular endothelial cells to fluid shear stress. *J. Biomech. Eng.* 103:177-185.
- Ettenson, D. S., and A. I. Gotlieb. 1992. Centrosomes, microtubules, and microfilaments in the reendothelialization and remodeling of double-sided in vitro wounds. *Lab. Invest.* 66:722-733.
- Fox, J. E. B. 1985. Linkage of a membrane skeleton to integral membrane glycoproteins in human platelets. *J. Clin. Invest.* 76:1673-1683.
- Fung, Y. C., and S. Q. Liu. 1993. Elementary mechanics of the endothelium in blood vessels. *J. Biomech. Eng.* 115:1-12.
- Gibson, L. J., and M. F. Ashby. 1988. *Cellular Solids: Structure and Properties*. Pergamon Press, Oxford.
- Gorlin, J. B., R. Yamin, S. Egan, M. Stewart, T. P. Stossel, D. J. Kwiatkowski, and J. H. Hartwig. 1990. Human endothelial actin-binding protein: a molecular leaf spring. *J. Cell Biol.* 111:1089-1105.
- Gotlieb, A., B. Langille, M. Wong, and D. Kim. 1991. Biology of disease: structure and function of the endothelial cytoskeleton. *Lab. Invest.* 65:123.
- Harrigan, T. P. 1990. Transduction of stress to cellular signals. First World Congress of Biomechanics, University of California, San Diego, Vol. 2. 51. (Abstr.)
- Hartwig, J. H., K. A. Chambers, and T. P. Stossel. 1989. Association of gelsolin with actin filaments and cell membranes of macrophages and platelets. *J. Cell Biol.* 108:467-479.
- Hartwig, J. H., K. S. Zaner, and P. A. Janmey. 1988. The cortical actin gel of macrophages. In *Cell Physiology of Blood*. Rockefeller University Press, New York. 126-140.
- Ito, J., K. S. Zaner, and T. P. Stossel. 1987. Nonideality of volume flows and phase transitions of F-actin solutions in response to osmotic stress. *Biophys. J.* 51:745-753.
- Janmey, P. A., U. Euteneuer, P. Traub, and M. Schliwa. 1991. Viscoelastic properties of vimentin compared with other filamentous biopolymer networks. *J. Cell Biol.* 113:155-160.
- Janmey, P. A., S. Hvidts, J. Kas, D. Levche, A. Megg, E. Sackman, M. Schliwa, and T. P. Stossel. 1994. The mechanical properties of actin gels. *J. Biol. Chem.* 269:32503-32513.
- Kerst, A., C. Chmielewski, C. Livesay, R. E. Buxbaum, and S. R. Heidemann. 1990. Liquid crystal domains and thixotropy of filamentous actin suspensions. *Proc. Natl. Acad. Sci. USA*. 87:4241-4245.
- Kishino, A., and A. Yanagida. 1988. Force measurements by micro manipulation of a single actin filament by glass needles. *Nature*. 334:74-76.
- Kolodney, M. S., and R. B. Wysolmerski. 1992. Isometric contraction by fibroblasts and endothelial cells in tissue culture: a quantitative study. *J. Cell Biol.* 117:73-82.
- Kreis, T. E., and W. Birchmeier. 1980. Stress fiber sarcomeres of fibroblasts are contractile. *Cell*. 22:555.
- Levesque, M. J., D. Liepsch, S. Moranec, and R. M. Nerem. 1986. Correlation of endothelial cell shape and wall shear stress in a stenosed dog aorta. *Arteriosclerosis*. 6:220-229.
- Lewis, W. H., and M. R. Lewis. 1924. Behavior of cells in tissue cultures. In *General Cytology*, E. V. Condy, editor. University of Chicago Press, Chicago. 385-447.
- Lux, S. E. 1979. Dissecting the red-cell membrane skeleton. *Nature*. 281:426.
- Nossal, R. 1988. On the elasticity of cytoskeletal networks. *Biophys. J.* 43:349-359.
- Osawa, F. 1977. Actin-actin bond strength and the conformational change of F-actin. *Biorheology*. 14:11-19.
- Resnick, N., T. Collins, W. Atkinson, D. Bonthron, C. F. Dewey, and M. A. Gimbrone. 1993. Platelet derived growth factor  $\beta$  chain promoter contains a cis-acting fluid shear-stress responsive element. *Proc. Natl. Acad. Sci. USA*. 90:4591-4595.
- Runge, M. S., T. M. Laue, D. A. Yphantis, M. Lifshits, A. Saito, K. Altin, K. Reinke, and R. C. Williams. 1981. ATP-induced formation of an associated complex between microtubules and neurofilaments. *Proc. Natl. Acad. Sci. USA*. 78:1431-1435.
- Sachs, F. 1988. Mechanical transduction in biological systems. *Crit. Rev. Biomed. Eng.* 16:146-169.
- Satcher, R. L. 1993. A mechanical model of vascular endothelium. Ph.D. thesis. Massachusetts Institute of Technology, Cambridge, MA.
- Satcher, R. L., S. R. Bussolari, M. A. Gimbrone, and C. F. Dewey. 1992. The distribution of fluid forces on model arterial endothelium using computational fluid dynamics. *J. Biomech. Eng.* 114:309-316.
- Sato, M., M. Levesque, and R. Nerem. 1987. An application of the micropipette technique of culture bovine aortic endothelial cells. *J. Biomech. Eng.* 109:27-34.
- Shen, J., F. Lusinskas, C. F. Dewey, and M. A. Gimbrone. 1992. Fluid shear stress modulates cytosolic free calcium in vascular endothelial cells. *Am. J. Physiol.* 262:C384-C390.
- Stossel, T. P. 1988. The mechanical responses of white blood cells. In *Inflammation: Basic Principles and Clinical Correlates*. J. I. Gallin, I. M. Goldstein, and R. Synderon, editors. Raven Press, New York. 325-342.
- Sumpio, B. E., W. Du, C. R. Cohen, L. Evans, C. Isales, O. R. Rosales, and I. Mills. 1993. Signal transduction pathways in vascular cells exposed to cyclic strain. In *Biomechanics and Cells*. F. Lyall, A. J. El Haj, editors. Cambridge University Press, Cambridge. 1-22.
- Suzuki, A., M. Yamazaki, and T. Ito. 1989. Osmoelastic coupling in biological structures: formation of parallel bundles of actin filaments in a crystalline-like structure caused by osmotic stress. *Biochemistry*. 28:6513-6518.
- Taniguchi, M., and V. Kamiya. 1983. Morphological changes and crystal structure of skeletal muscle actin. *Nuclear Instr. Methods*. 208:541-544.
- Theret, D. P., M. J. Levesque, M. Sato, R. M. Nerem, and L. T. Wheeler. 1988. The application of a homogeneous half-space model in the analysis of endothelial cell micropipette measurements. *J. Biomech. Eng.* 110:190-199.
- Wang, W., J. P. Butler, and D. E. Ingber. 1994a. Control of cytoskeletal mechanics by extracellular matrix, cell shape, and mechanical tension. *Biophys. J.* 66:2181-2189.
- Wang, W., J. P. Butler, and D. E. Ingber. 1994b. Mechanotransduction across the surface and through the cytoskeleton. *Science*. 260:1124-1127.
- White, G., M. A. Gimbrone, and K. Fujiwara. 1983. Factors influencing the expression of stress fibers vascular endothelial cells, in situ. *J. Cell Biol.* 97:416-424.